

Generic behavior of coupled oscillators

T. Hogg

Physics Department, Stanford University, Stanford, California 94305

B. A. Huberman

Xerox Palo Alto Research Center, Palo Alto, California 94304

(Received 23 May 1983)

There exist a number of interesting physical problems, such as the ac-driven, dc SQUID (superconducting quantum interference device) or convection in conducting fluids, which can be described by the dynamics of driven coupled oscillators. In order to study their behavior as a function of coupling strength and nonlinearity, we have considered the dynamics of two coupled maps belonging to the same universality class as the oscillators. We have analytically determined some of the parameter values for which they exhibit locked states as well as bifurcations into aperiodic behavior. Furthermore, we found a set of codimension-two bifurcations into quasiperiodic orbits near which the rotation number becomes vanishingly small. These bifurcations are characterized by the existence of periodic regimes interrupted by episodes of phase slippage. Finally, we show the effect of thermal fluctuations on the bifurcation diagram by computing the Lyapunov exponent in the presence of external and parametric noise.

I. INTRODUCTION

There exist a number of interesting physical problems, such as ac-driven dc SQUIDS (superconducting quantum interference devices),¹ or convection in conducting fluids, which can be described by the dynamics of driven coupled oscillators. In particular, recent experiments on the magnetohydrodynamics of mercury in small-aspect-ratio Bénard cells² show the existence of quasiperiodic motions in addition to the now familiar repertoire of periodic and chaotic phenomena. Since small-aspect-ratio experiments are essentially probing the behavior of systems with very few degrees of freedom, the appearance of irrationally related frequencies indicates the existence of locking-unlocking transitions in simple nonlinear oscillators. This problem is also relevant to neurodynamics³ and chemical reactions,⁴ where it becomes important to understand the global dynamics of coupled systems as a function of both nonlinearity and coupling strength.

To address some of these issues, we have considered the dynamics of two coupled maps belonging to the same universality class as period-doubling oscillators. We have analytically determined some of the parameter values for which they exhibit locked states as well as their bifurcations into aperiodic behavior. Furthermore, we found a set of codimension-two bifurcations into quasiperiodic orbits near which the rotation number becomes vanishingly small. These bifurcations are characterized by the existence of periodic regimes interrupted by episodes of phase slippage. We also studied the effects of thermal fluctuations on the transition to chaos by computing the Lyapunov exponent in the presence of noise. We discovered that the addition of external or parametric noise leads to a blurring of the fine-scale locking-unlocking bifurcation structure found in the absence of

noise. Finally, the universality of our results was tested by examining other types of coupled maps exhibiting period-doubling bifurcations.⁵

II. COUPLED MAPS

In this section we first discuss techniques that can be used to characterize orbits of discrete maps as periodic, quasiperiodic, or chaotic. These methods are then applied to investigate the effect of coupling two period-doubling maps.

Consider the general vector mapping

$$\vec{x}_{n+1} = \vec{F}(\vec{x}_n), \quad n=0,1,\dots \quad (2.1)$$

and its N th iterate $\vec{F}^{(N)}(\vec{x}) \equiv \vec{F}^{(N-1)}(\vec{F}(\vec{x}))$ with $\vec{F}^{(1)}(\vec{x}) \equiv \vec{F}(\vec{x})$. The asymptotic behavior of a series of iterates of the map can be characterized by the largest Lyapunov exponent which, for an initial point \vec{x}_0 in an attracting region, is defined to be

$$\lambda = \lim_{N \rightarrow \infty} \{ \ln[|\underline{D}^{(N)}(\vec{x}_0)|] / N \}, \quad (2.2)$$

where $|\underline{D}^{(N)}|$ is the norm⁶ of the derivative matrix

$$D_{ij}^{(N)}(\vec{x}) = \frac{\partial F_i^{(N)}(\vec{x})}{\partial x_j}. \quad (2.3)$$

This exponent measures how rapidly two nearby orbits in an attracting region converge or diverge. It can be evaluated by noting that $\underline{D}^{(N)}(\vec{x}_0) = \underline{D}^{(N-1)}(\vec{F}(\vec{x}_0))\underline{D}(\vec{x}_0)$; so if $\vec{x}_0, \vec{x}_1, \vec{x}_2, \dots$ are successive iterates of the map, then

$$\underline{D}^{(N)}(\vec{x}_0) = \underline{D}(\vec{x}_{N-1}) \cdots \underline{D}(\vec{x}_1)\underline{D}(\vec{x}_0). \quad (2.4)$$

In practice, λ is computed by initially iterating the map many times to eliminate transient behavior and then using

a large number N of successive points to compute the derivative matrix as indicated in Eq. (2.4). Finally, the quantity $\ln[||\underline{D}^{(N)}(\bar{x}_0)||]/N$ is used as an approximate value of the Lyapunov exponent for this attracting region.⁷

This exponent provides a way to distinguish among periodic, quasiperiodic, and chaotic motion. Specifically, if \bar{x}_0 is part of a stable periodic orbit of length K , then the norm of the derivative matrix, $||\underline{D}^{(K)}(\bar{x})||$, will be less than one for every \bar{x} in the K cycle. Thus the exponent will be negative and characterize the rate at which small perturbations from the fixed cycle decay. A zero value for the exponent indicates quasiperiodic behavior in which nearby paths maintain their distance on the average. And finally, when λ becomes positive, nearby points in the attracting region diverge from each other giving chaotic motion. In general the exponent will depend on the initial point used in the iteration because there may be several stable attractors each with a separate basin of attraction.

We now use these techniques to examine the effect of coupling two nonlinear maps that display period doubling. In particular, consider the two-dimensional mapping

$$x_{n+1} = rx_n(1-x_n) + \epsilon(y_n - x_n), \quad (2.5a)$$

$$y_{n+1} = ry_n(1-y_n) + \epsilon(x_n - y_n), \quad (2.5b)$$

where the nonlinearity parameter r is such that $0 \leq r \leq 4$ and the coupling constant ϵ satisfies $0 \leq \epsilon \leq 1$. This map displays a wide range of behavior as the parameters r and ϵ are varied including periodic, quasiperiodic, and chaotic motion. Note that the derivative matrix \underline{D} of Eq. (2.5) at the point (x, y) is given by

$$\underline{D}(x, y) = \begin{bmatrix} r - \epsilon - 2rx & \epsilon \\ \epsilon & r - \epsilon - 2ry \end{bmatrix}. \quad (2.6)$$

Figure 1 shows some of the stable behaviors for various r and ϵ values. Along the horizontal axis, where $\epsilon = 0$, one sees the familiar period-doubling sequence of the one-dimensional logistic map. The boundaries of the stable regions for the low periods have been computed analytically by determining where the norm of the corresponding derivative matrix equals one. The quasiperiodic and chaotic regions were determined by measuring the Lyapunov exponent. In-phase periods mean $x = y$ for the fixed cycle. Out-of-phase period 2 is the case for which (a, b) becomes (b, a) under a single iteration of the map and returns to (a, b) after two iterations with $a \neq b$. Similarly, the out-of-phase period 4 has $(a, c) \rightarrow (b, d) \rightarrow (c, a) \rightarrow (d, b) \rightarrow (a, c)$ under successive iterations of the map with $a \neq c$ and $b \neq d$.

In particular, the norm of the derivative matrix shows that there is a stable fixed point for the region in which $r < 3 - 2\epsilon$. The in-phase 2 cycle is stable for

$$1 + 2(1 + \epsilon + \epsilon^2)^{1/2} \leq r \leq 1 + 6^{1/2} = 3.449 \quad (2.7)$$

with $\epsilon \leq (3^{1/2} - 1)/2 = 0.37$. Similarly, the out-of-phase case is stable for

$$3 - 2\epsilon \leq r \leq 1 + (6 - 10\epsilon + 4\epsilon^2)^{1/2}. \quad (2.8)$$

Note that these regions overlap, indicating that the cou-

pled maps have multiple basins of attraction for some parameter values.

For nonzero values of the coupling constant, instead of simple period doubling, successive periods can be separated by regions of quasiperiodic motion in which the frequencies of the two oscillators are incommensurate. These transition regions also contain various locked orbits of high period, including asymmetric periods in which x and y cycle over distinct sets of values.

A more detailed picture of this map can be obtained by investigating the behavior along a cross section of the phase diagram. Specifically, we chose the value $\epsilon = 0.06$ which gives typical results for this map. A bifurcation diagram for a particular choice of initial conditions ($x = 0.2, y = 0.4$) is given in Fig. 2. This figure was obtained by starting with $r = 3$ and incrementing in small steps up to $r = 4$. At each new r value the final (x, y) iterate of the previous value was used as the initial point. This corresponds to continuously changing the system's parameters without restoring the original state of the system. The behavior of the Lyapunov exponent for two different initial conditions is shown in Fig. 3 for r in the range 3.0–3.7 and $\epsilon = 0.06$. The value of the second Lyapunov exponent⁶ for these parameters is so close to that of the largest exponent that they are not distinguish-

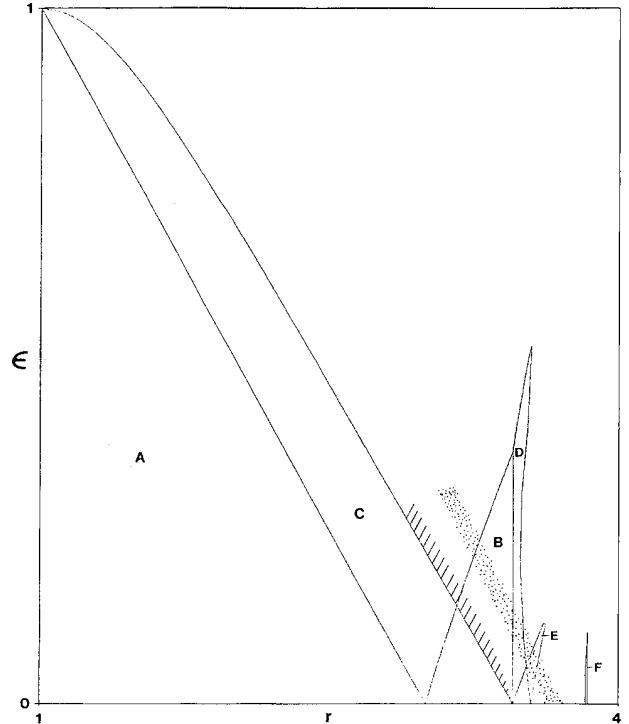


FIG. 1. Some of the parameter domains where stable attractors exist for the coupled maps as a function of nonlinearity parameter r and coupling ϵ . Regions are A, period 1; B, in-phase, period 2; C, out-of-phase, period 2; D, in-phase, period 4; E, out-of-phase, period 4; and F, period 3. Dashed region is quasiperiodic motion and the dotted one corresponds to chaotic motion.

able on the scale of the plot. Note that for some values of the parameters the two attracting regions are not of the same type. For instance, when $r=3.38$ and $\epsilon=0.06$ there is both a periodic and a quasiperiodic attractor. Sudden transitions between basins of attraction can be seen in the plot of the exponent. We should note that the size of an attracting region varies with the parameter values and becomes very small when near the stability boundary.

In addition to the periodic and chaotic behavior seen in the uncoupled ($\epsilon=0$) case, the coupled map displays quasiperiodic motion. In particular, the plot of the exponent in Fig. 3(b) shows that the transition from out-of-phase period 2 to 4 is separated by a quasiperiodic region in which the exponent is zero, as well as a chaotic region with positive exponent. The detailed transition out of the quasiperiodic region involves a complicated series of periodic orbits as shown in Fig. 4 which shows the behavior of the exponent in the transition region.

Many successive frequency lockings with high periods appear before the period-4 orbits. Plots of the iterates of the map and their power spectra for a locked periodic orbit and nearby quasiperiodic motion are given in Figs. 5 and 6, respectively. Note that the iterates of the map in this region actually form two groups of points located symmetrically around the diagonal $x=y$. For clarity, only one of these groups is actually shown in the figure. The fundamental frequency in Fig. 5 is 1.111×10^{-2} corresponding to a period-90 orbit. The appearance of additional frequencies, characteristic of quasiperiodic behavior, can be seen in the power spectrum of Fig. 6(b). Specifically, a set of fundamental frequencies is 1.087×10^{-2} , 0.2554, and 0.5. It should also be pointed out that the various ratios of these three frequencies change continuously when r is changed slightly from the

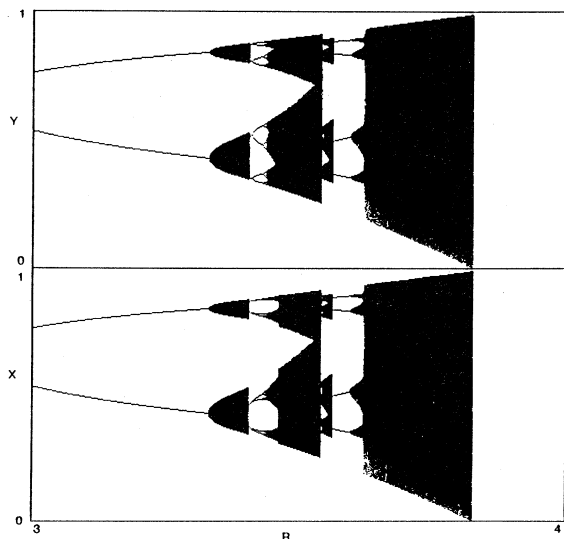


FIG. 2. Bifurcation diagram for the coupled maps with r ranging from 3 to 4 and $\epsilon=0.06$. For each value of r , we used the final point of the previous r value and 1500 iterates are plotted. This shows the period-doubling sequence as well as quasiperiodic and chaotic regions.

value of 3.39 used in the figure. By comparison, Fig. 7 shows the iterates and the power spectrum of a particular chaotic orbit. In this case the spectrum has a broadband component and the iterates form four similar groups of points, only one of which is shown in the figure.

This behavior is characteristic of a codimension-two bifurcation which displays different transitions in different directions of parameter space. In particular, when

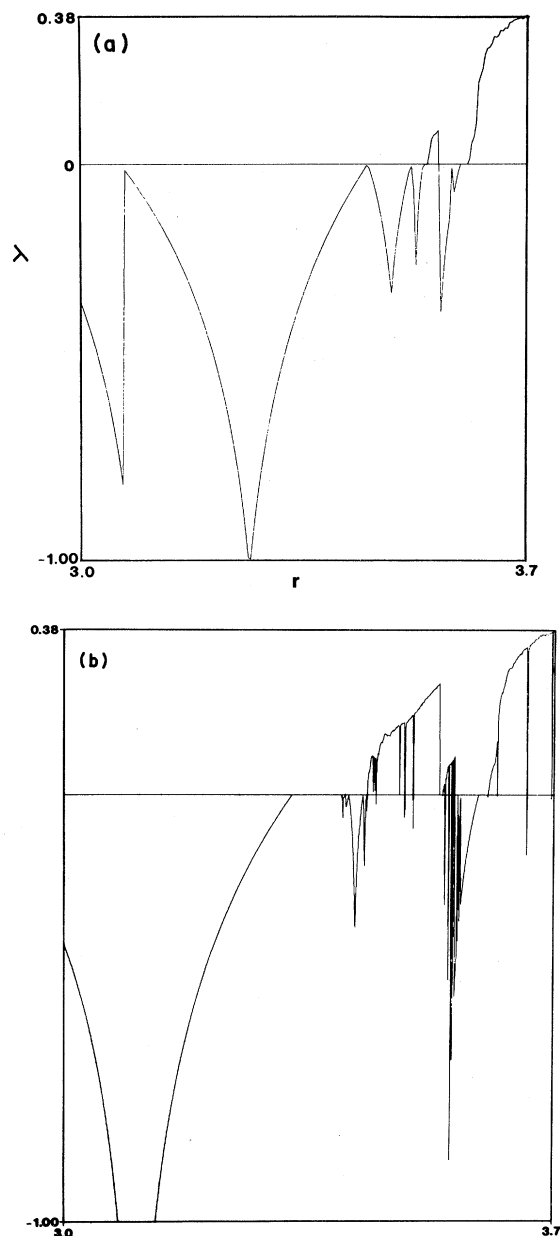


FIG. 3. Lyapunov exponent for the coupled maps as a function of r ranging from 3.0 to 3.7 and with $\epsilon=0.06$. Each point was obtained by iterating many times from the initial condition to eliminate transient behavior and then averaging over another 50 000 iterations. Initial conditions: (a) $x=0.2$, $y=0.25$, with 200 r values; (b) $x=0.2$, $y=0.4$, with 1000 r values.

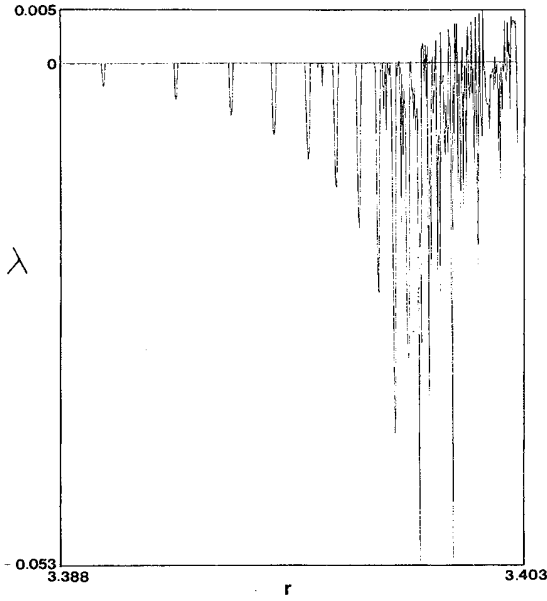


FIG. 4. Detailed structure of the Lyapunov exponent for the transition from quasiperiodic behavior to a 4 cycle. This is an expanded version of Fig. 3(b) with r varying between 3.388 and 3.403. Plot consists of 501 r values each of which was obtained by iterating 100 000 times from the initial condition and then averaging over another 50 000 iterations.

$r = 1 + 6^{1/2}$ and $\epsilon = 0$, an increase in r results in the period 2 to period 4 bifurcation of the uncoupled map. An increase in ϵ , on the other hand, produces quasiperiodic motion. This behavior is also seen for the higher period transitions. A further increase in the coupling strength can lead to chaotic motion. Alternatively, an increase in coupling strength reduces the nonlinearity value for the onset of chaos.

For the particular case of the transition into chaos through locking-unlocking transitions, Kaneko has shown that the parameter values at which the lockings take place obey the same scaling relations as those found in circle maps,⁸ i.e.,

$$r_\infty - r_n \propto n^{-2} \quad (2.9)$$

for large n , where r_n is the value of the nonlinearity parameter at which the period $8n - 1$ appears and r_∞ is the limit of r_n as $n \rightarrow \infty$.

Before concluding this section, we mention an interesting phenomenon that is observed near the transition into quasiperiodic behavior. It consists of phase-locked periodic behavior for some time, interrupted by episodes of phase slips between the entrained states. This leads to time sequences consisting of periodic oscillations, interrupted by kinks in the phase of the systems. This behavior, which has been observed in some chemical oscillators,⁹ becomes more irregular with increasing ϵ , leading to the fully unlocked regime described above.

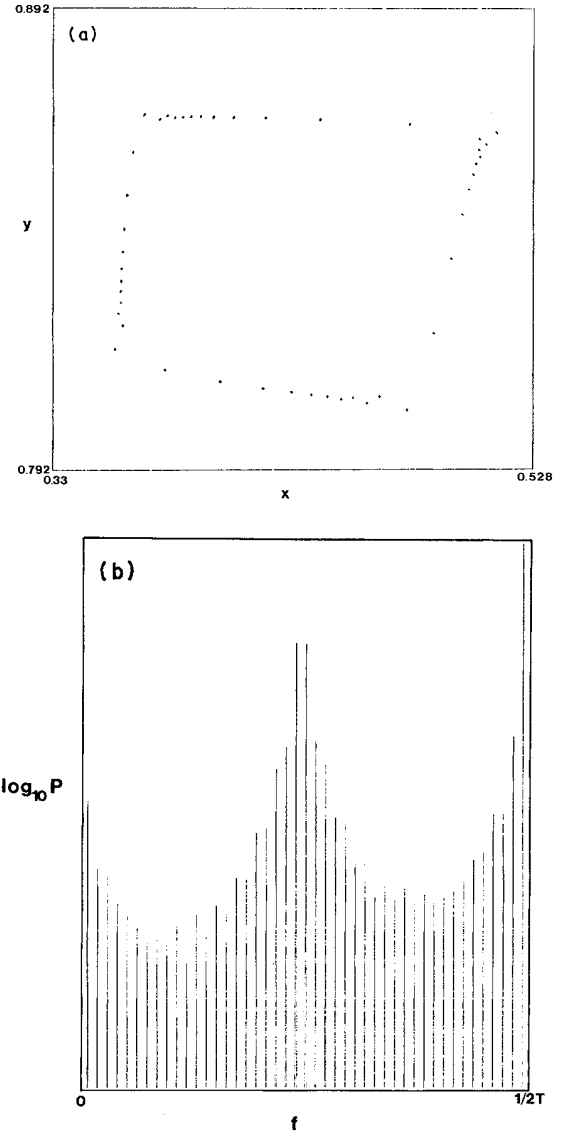


FIG. 5. Frequency locking during the quasiperiodic to 4 cycle transition for $r = 3.38932$, $\epsilon = 0.06$, and the initial point $x = 0.2, y = 0.4$. (a) Plot of the iterates of the map (x_n, y_n) ; (b) power spectrum of the x_n computed by first iterating the map 20 000 times to eliminate transients and then using 8192 samples. The dc term has been removed from the spectrum.

III. THE EFFECT OF FLUCTUATIONS

In this section we investigate the behavior of the coupled maps in the presence of thermal fluctuations or other noise. As has been shown in the case of uncoupled nonlinear oscillators, the addition of external or parametric fluctuations has a pronounced effect on the dynamics of such systems.¹⁰ In particular, the presence of noise introduces a gap in the bifurcation sequence of period-doubling systems and renormalizes the threshold for the appearance of chaotic behavior. It is therefore of interest to investi-

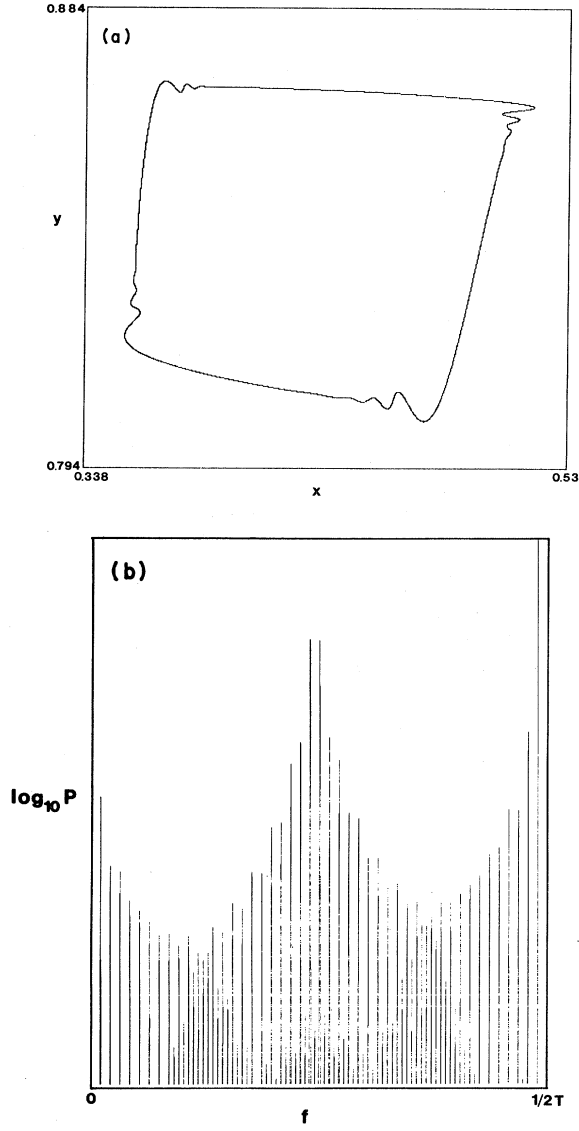


FIG. 6. Quasiperiodic motion for $r=3.39$, $\epsilon=0.06$, and initial point $x=0.2, y=0.4$. (a) Plot of the iterates of the map (x_n, y_n) ; (b) power spectrum of the x_n with the dc term removed.

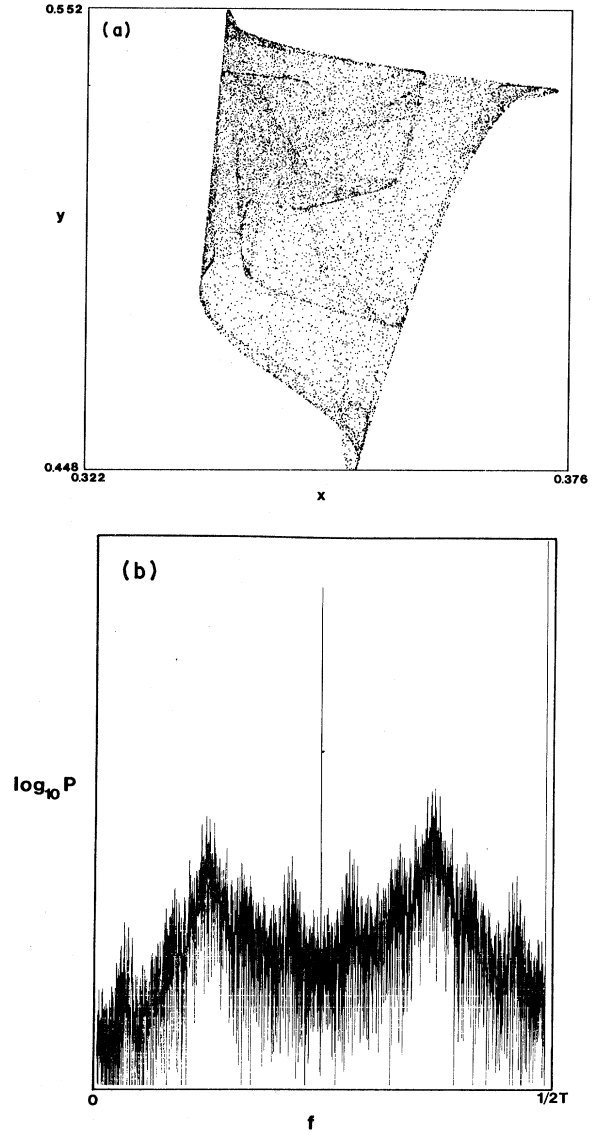


FIG. 7. Chaotic motion for $r=3.615$, $\epsilon=0.06$, and initial point $x=0.2, y=0.4$. (a) Plot of the iterates of the map (x_n, y_n) ; (b) power spectrum of the x_n with the dc term removed.

gate the effects of noise on the locking-unlocking behavior of coupled oscillators.

The effect of noise was modeled by adding uniformly distributed random numbers to the map of Eq. (2.5). Specifically, we considered the map

$$x_{n+1} = rx_n(1-x_n) + \epsilon(y_n - x_n) + \sigma\delta_n^{(1)}, \quad (3.1a)$$

$$y_{n+1} = ry_n(1-y_n) + \epsilon(x_n - y_n) + \sigma\delta_n^{(2)}, \quad (3.1b)$$

where $\delta_n^{(1)}$ and $\delta_n^{(2)}$ are random numbers uniformly distributed in the interval $[-1, 1]$ and σ is the amplitude of the noise. These fluctuations destroy the fine scale detail of the transitions and the quasiperiodic regions. Furthermore, the r value at which the exponent first becomes positive shifts downward. Figure 8 shows the effect of a

small amount of noise on the fine scale structure of the Lyapunov exponent for the same parameter values used in Fig. 4, namely, $3.388 \leq r \leq 3.403$, $\epsilon=0.06$, and the initial point $(0.2, 0.4)$.

An additional case occurs when the parameters of the oscillators have small, random variations due, for instance, to external noise. These so-called parametric fluctuations can be simulated by modulating the values of the nonlinearity parameters by uniform random numbers in a small interval. This gives the following map:

$$x_{n+1} = r_n^{(1)} x_n(1-x_n) + \epsilon(y_n - x_n), \quad (3.2a)$$

$$y_{n+1} = r_n^{(2)} y_n(1-y_n) + \epsilon(x_n - y_n), \quad (3.2b)$$

where $r_n^{(1,2)} = r(1 + \sigma\delta_n^{(1,2)})$ and again the $\delta_n^{(1)}$ and $\delta_n^{(2)}$ are

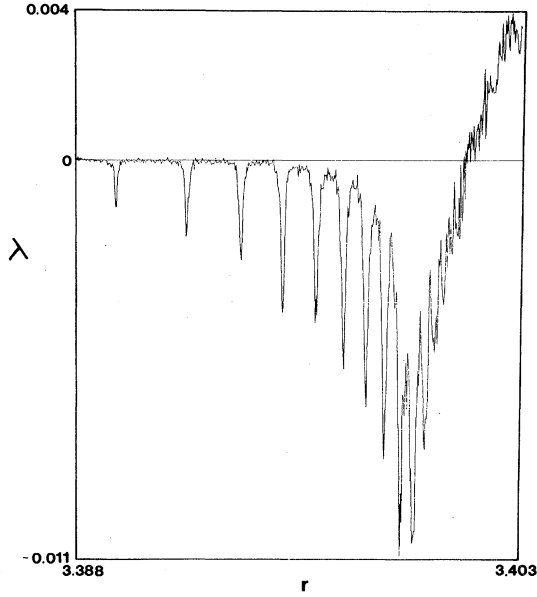


FIG. 8. Effect of additive noise on the fine scale structure of the Lyapunov exponent for the same parameter values as used in Fig. 4. Here the noise amplitude is $\sigma=0.00005$. Plot consists of 501 r values each of which was obtained by iterating 100 000 times from the initial condition and then averaging over another 50 000 iterations.

independent random numbers uniformly distributed in $[-1,1]$. The effect of such parametric variations is similar to that of simple additive noise in that the fine details of the transition are lost.

IV. GENERALIZATIONS

The preceding discussion considered the effect of coupling two identical maps. However, it is also of interest to examine the case in which the nonlinearity parameters are unequal, corresponding to the coupling of two different oscillators. Specifically, we considered the map

$$x_{n+1} = r^{(1)}x_n(1-x_n) + \epsilon(y_n - x_n), \quad (4.1a)$$

$$y_{n+1} = r^{(2)}y_n(1-y_n) + \epsilon(x_n - y_n) \quad (4.1b)$$

with $r^{(1)} \neq r^{(2)}$. The general kind of behavior seen is similar to the previous case, that is, the coupling produces a new quasiperiodic motion and can lead to chaos. This can be seen in the bifurcation diagram of Fig. 9 which displays the behavior of Eqs. (4.1) for $r^{(1)}=3.1$, $r^{(2)}=2.4$, and with $0 \leq \epsilon \leq 0.5$.

Finally, the behavior discussed in the previous sections is not limited to the particular form of the map given by Eq. (2.5). For instance, very similar behavior was seen for the coupled system

$$x_{n+1} = r \sin(\pi x_n) + \epsilon(y_n - x_n), \quad (4.2a)$$

$$y_{n+1} = r \sin(\pi y_n) + \epsilon(x_n - y_n) \quad (4.2b)$$

with r , x , and y in the interval $[0,1]$. This suggests that

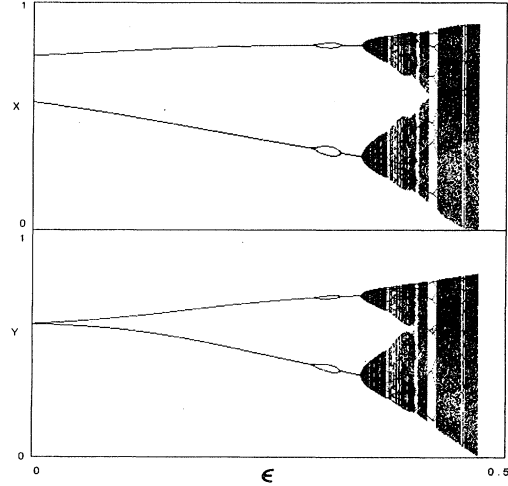


FIG. 9. Bifurcation diagram for the map of Eqs. (4.1) with $r^{(1)}=3.1$, $r^{(2)}=2.4$, and $0 \leq \epsilon \leq 0.5$. For each value of ϵ , the map was iterated 500 times from the initial point $x=0.4, y=0.2$ to eliminate transients, and the next 500 iterates were plotted.

the qualitative features of the behavior of Eq. (2.5) are universal and will be seen in any map with a quadratic maximum. Furthermore, other forms of coupling, such as using ϵy and ϵx instead of $\epsilon(y-x)$ and $\epsilon(x-y)$, respectively, in Eq. (2.5),³ also produce the behavior seen here.

V. CONCLUSION

We have seen some general features of coupled maps that individually display period-doubling bifurcation cascades into chaos. A new kind of behavior that is not seen in the uncoupled case is quasiperiodic motion with complicated transitions which include period lockings. These transitions are smoothed by additive or parametric noise. The various types of behavior can be distinguished experimentally in the power spectra. In particular, new peaks that come in halfway between old ones as parameters are varied indicate period doubling. Quasiperiodic motion is characterized by groups of irrationally related frequencies that shift continuously with respect to each other for small changes in the parameters. Finally, chaotic motion has a broadband spectrum, which in many cases also contains sharp superimposed peaks.

Finally we should note that the connection of this discussion to experimental results requires a careful consideration of hysteresis effects. In actual experiments the system's parameters are often adjusted continuously without restoring the system to the same initial conditions for each new parameter value. Thus transient behavior can be important in relation to how fast the parameters are varied during an experiment. Hysteresis will be especially important when the convergence of the system to the attracting region is slow, i.e., when both exponents are near zero, which is the case for the regions of quasiperiodic motion displayed by the coupled maps. To investigate these problems, we have computed the asymptotic behavior of the coupled maps as parameters are varied by

using the final point after a given number of iterations with a particular parameter value as the initial point for the next value.

We conclude by mentioning that the effects we have discussed are likely to be encountered in simulations of the actual differential equations describing coupled oscillators. In particular, our own experience with the equations describing an ac-driven, dc SQUID showed that, in the period-doubling regime, the phase diagrams obtained by numerical integration of the coupled equations are in

qualitative agreement with those of the coupled maps. A better test, of course, would be provided by actual experiments on the real devices.

ACKNOWLEDGMENTS

This research was supported in part by Grant No. N00014-82-0699 from the U.S. Navy Office of Naval Research. T.H. would also like to thank the Xerox Palo Alto Research Center for a fellowship.

¹See, for example, *Introduction to Superconductivity*, edited by A. C. Rose-Innes and E. H. Rhoderick (Pergamon, Oxford, 1978).

²A. Libchaber and S. Fauve, in *Melting, Localization, and Chaos*, edited by R. K. Kalia and P. Vashista (North-Holland, New York, 1982).

³R. King, B. A. Huberman, and J. Barchas, in *Synergetics of the Brain*, edited by H. Haken (Springer, Berlin, 1983).

⁴J. Neu, *SIAM J. Appl. Math.* **37**, 307 (1979).

⁵Some of our results have also been obtained by K. Kaneko (unpublished) and J. M. Yuan, M. Tung, D. H. Feng and L. Narducci (unpublished).

⁶The norm of the $N \times N$ matrix A is defined as $\|A\| \equiv \max_{\{\vec{v}\}} \{ |A\vec{v}| / |\vec{v}| \}$, where \vec{v} ranges over all nonzero N -vectors. The second Lyapunov exponent is computed by using the *minimum* value of $|A\vec{v}| / |\vec{v}|$, instead of

the norm.

⁷A. J. Lichtenberg and M. A. Liebermann, *Regular and Stochastic Motion*, Vol. 38 of *Applications of Mathematics in Science* (Springer, Berlin, 1983). Another method of computing the Lyapunov exponent for two-dimensional maps is given by S. D. Feit, *Commun. Math. Phys.* **61**, 249 (1978).

⁸K. Kaneko (unpublished). For the scaling properties of the circle map see K. Kaneko, *Prog. Theor. Phys.* **68**, 669 (1982); M. J. Feigenbaum, L. P. Kadanoff, and S. Shanker, *Physica* **5D**, 370 (1982); and D. Rand, S. Ostlund, J. Sethna, and E. Siggia, *Phys. Rev. Lett.* **49**, 132 (1982).

⁹M. Marek and I. Stuchl, *Biophys. Chem.* **3**, 241 (1975).

¹⁰For a review of the effect of fluctuations on chaotic dynamics see J. P. Crutchfield, D. Farmer, and B. A. Huberman, *Phys. Rep.* **92**, 45 (1982).